Active thermal cloak

Dang Minh Nguyen, Hongyi Xu, Youming Zhang, and Baile Zhang

Citation: Applied Physics Letters **107**, 121901 (2015); doi: 10.1063/1.4930989
View online: http://dx.doi.org/10.1063/1.4930989
View Table of Contents: http://scitation.aip.org/content/aip/journal/apl/107/12?ver=pdfcov
Published by the AIP Publishing

Active thermal cloak

Dang Minh Nguyen, Hongyi Xu,[1,a)] Youming Zhang,[1] and Baile Zhang[1,2,a)]
[1]*Division of Physics and Applied Physics, Nanyang Technological University, 21 Nanyang Link, Singapore 637371*
[2]*Centre for Disruptive Photonic Technologies, Nanyang Technological University, 21 Nanyang Link, Singapore 637371*

(Received 24 June 2015; accepted 28 July 2015; published online 21 September 2015)

Thermal cloaking, as an ultimate thermal "illusion" phenomenon, is the result of advanced heat manipulation with thermal metamaterials—heat can be guided around a hidden object smoothly without disturbing the ambient thermal environment. However, all previous thermal metamaterial cloaks were passive devices, lacking the functionality of switching on/off and the flexibility of changing geometries. In this letter, we report an active thermal cloaking device that is controllable. Different from previous thermal cloaking approaches, this thermal cloak adopts active thermoelectric components to "pump" heat from one side to the other side of the hidden object, in a process controlled by input electric voltages. Our work not only incorporates active components in thermal cloaking but also provides controllable functionality in thermal metamaterials that can be used to construct more flexible thermal devices. © *2015 AIP Publishing LLC*.
[http://dx.doi.org/10.1063/1.4930989]

The prospect of metamaterials in controlling various physical fields manifests itself in the research of creating invisibility phenomena that were unachievable with common materials. Cloaking for electromagnetic waves[1–15] and acoustic waves[16–19] has greatly stimulated, and benefited from, the development of electromagnetic and acoustic metamaterials. The recent concept of thermal cloaking,[20–27] similarly, has in turn spawn a new research field of thermal metamaterials, aiming at controlling heat at will. The first approach of realizing thermal cloaking followed the coordinate transformation method[20–23] ("transformation optics"[28,29]). The second approach adopted the scattering-cancellation method,[25,26] similar to previous plasmonic cloaking[1,7] and dc magnetic cloaking.[12,13] Both approaches of thermal cloaking, however, only apply to passive thermal metamaterials. Despite the fact that active components have already been incorporated in controllable electromagnetic and acoustic metamaterials for cloaking purposes,[6,13,18] thermal cloaking still lacks similar controllability.

In this letter, we propose and demonstrate an approach of active thermal cloaking with controllability. Different from previous approaches which are based on the manipulation of material's thermal properties, our work realizes active cloaking by "pumping" heat flux from one side to the other side of the cloak via thermoelectric (TE) components that are controlled by input electric voltages. The switching on/off of this active thermal cloak is demonstrated in the experiment. Another unique feature of this active cloak is that it can adapt to flexible geometries without redesigning its constituents. This flexibility of changing geometries is demonstrated by cloaking a circular object and a square object using the same thermoelectric components.

A schematic of the experiment is shown in Fig. 1(a). The first object to be hidden is a circular air hole with 32.0 mm radius embedded in a rectangular metal plate made of Carbon Steel (AISI 1050) with thermal conductivity of 49.8 $W\,m^{-1}\,K^{-1}$ and dimensions of $200.0 \times 100.0 \times 5.0$ mm. The 5.0 mm thickness is sufficiently thin to approximate the Carbon Steel plate as two dimensional object and is sufficiently thick to neglect the effect of convection. The center of the air hole is 40.0 mm away from the center of the Carbon Steel plate. This asymmetry of position will facilitate the observation of the cloaking effect, as will be shown later. To observe the cloaking effect, a diffusive heat flux is created by attaching a 60 °C hot surface (generated by a

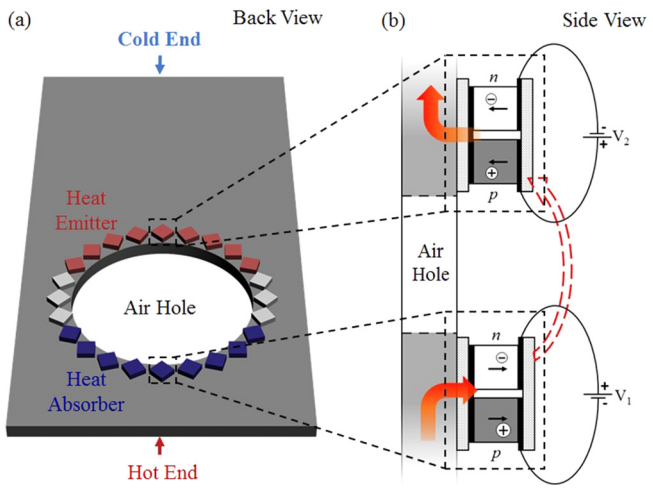

FIG. 1. Design of active thermal cloak. (a) Multiple TE components are arranged around the air hole with equal distance on the Carbon Steel plate. Blue TE components absorb incident thermal flux while red ones release heat back to the plate. In the demonstration, heat flows from bottom to top. As a result, grey TE components can stay inactive as they do not absorb or release heat, but they can be activated if heat flows in other directions. (b) The side view of the marked region in Fig. 1(a), illustrating the working mechanism of TE components when functioning as heat absorber/emitter. An applied voltage causes a directional motion of charge carriers in p/n blocks, resulting in a heat flux in the designed direction. The bottom/top orange arrow indicates the absorption/release of heat by TE components. The dashed arrow indicates the heat transfer through a constant-temperature heat "reservoir" which is a large copper bulk in the experiment.

[a)]Authors to whom correspondence should be addressed. Electronic addresses: HYXU@ntu.edu.sg and BLZHANG@ntu.edu.sg.

constant temperature heater) at the lower end of the Carbon Steel plate, and a 0 °C cold surface (created by an ice-water tank) at the upper end of the Carbon Steel plate. Temperature profile of the system is captured by an infrared camera FLIR ®T620. To correct the low emissivity of Carbon Steel, a black vinyl electrical insulation tape with emissivity of around 0.95 is used to cover its surface. NTE424 thermal compound is applied at every thermal contact to reduce thermal impedance.

The key to realizing active thermal cloaking is to "pump" the heat flux incident on one side of the cloak to the other side precisely. In our demonstration, this is realized with 24 TE components (each with dimensions of $6.0 \times 6.0 \times 3.8$ mm, manufactured by Global Component Sourcing) uniformly spaced around the air hole. Each TE component is controlled with an external input voltage to absorb or release heat. Heat absorbed by the TE components (located near the hot end of the Carbon Steel plate; as marked in blue in Fig. 1(a)) is dissipated into a constant-temperature heat "reservoir" (a large copper bulk attached to these TE components; not shown in the figure), and heat released from the TE components (located near the cold end of the Carbon Steel plate; as marked in red in Fig. 1(a)) is also provided by the same heat "reservoir." The dashed arrow indicated in Fig. 1(b) implies that the constant-temperature heat "reservoir" provides a channel for heat to be pumped from one side to the other side of the cloak. When the cloak is switched on, all TE components are applied with different electric voltages to absorb/release the exact amounts of heat accordingly to recover the system from temperature distortion. It should be noted that, when pumping the heat, the TE components also consume energy and will generate extra heat. Therefore, the heat "reservoir" will receive more heat than it will release. Ideally, this extra heat can be "pumped" to an additional heat channel and be dissipated elsewhere. Here, we just leave it to be dissipated from the heat "reservoir" via air convection.

For the electric controlling part, each TE component is connected to a dc-dc buck converter (a mini voltage controller device) to control its input current. This input current can be determined by solving the cooling capacity equation[30] for TE components functioning as heat absorber

$$Q_L = \alpha I T_L - \frac{1}{2} I^2 R - \kappa_T (T_H - T_L). \quad (1)$$

As for TE components functioning as heat releaser, the heat rejection equation[30] is used

$$Q_H = \alpha I T_H + \frac{1}{2} I^2 R - \kappa_T (T_H - T_L). \quad (2)$$

In Equations (1) and (2), I is the input current, Q_L and Q_H are the amount of heat absorbed/released by each TE component. Its high/low temperature surfaces are denoted as T_H/T_L, respectively. The three representative parameters of a TE components are α—Seebeck coefficient, R—Electrical resistance, and κ_T—Thermal conductance. Knowing the required amount of heat absorbed/released, as well as the targeted temperature profile, one can solve Equation (1) or (2) to obtain the input current for each TE component. In our calculation, the effective Seebeck coefficient, electrical resistance, and thermal conductance of a TE component are $3.4 \times 10^{-3}\,\Omega\,\mathrm{T}^{-1}$, $0.041\,\Omega$, and $0.095\,\mathrm{W\,K}^{-1}$, respectively. In our experiment, the amount of heat absorbed/released is pre-calculated based on prior knowledge about hot end/cold end temperature. However, conceptually, for a non-predetermined setup, the cloak can still function properly by using a thermal camera to measure the boundary temperatures of the system, which will subsequently be used to obtain the amount of heat involved.

Now we demonstrate the effectiveness of the active thermal cloak. For comparison, we first consider a solid Carbon Steel plate without any hole embedded. As shown in Fig. 2(a), after about 10 min for heat to diffuse from bottom to top, a homogeneous temperature profile is formed on the Carbon Steel plate. When an air hole is present, as shown in Fig. 2(b), this air hole will block the heat channel and distort

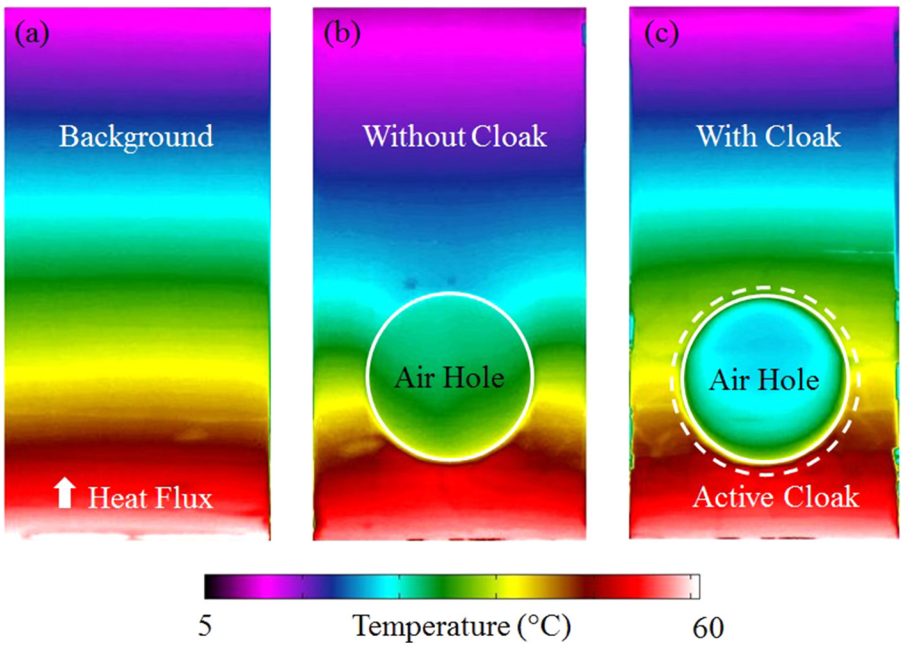

FIG. 2. Realization of thermal invisibility of a circular air hole in a metal plate. (a) Thermal image of a complete Carbon Steel plate without any air hole. Heat flux diffuses from bottom to top, forming a homogeneous temperature profile. (b) Distorted temperature profile caused by an embedded circular air hole. (c) Restored homogeneous temperature profile when the cloak is cloaking the air hole. The dashed circle indicates the position of TE components.

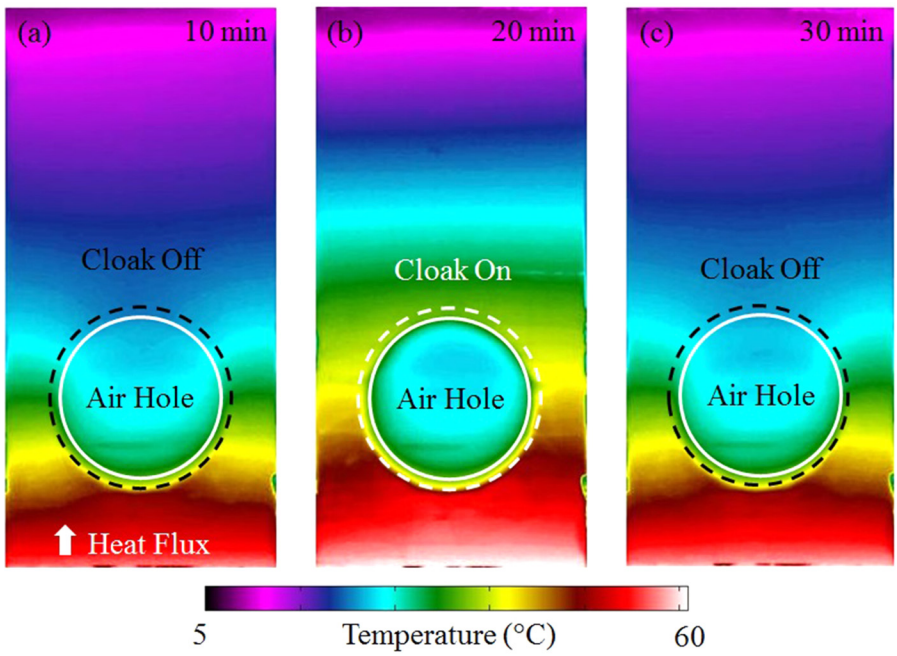

FIG. 3. Dynamic switching of the cloaking function. (a) Distorted temperature profile when the cloak is not in operation. Heat flux diffuses from bottom to top. (b) Thermal invisibility achieved when the cloak is activated. (c) Temperature distortion is restored when the cloak is deactivated. In each stage, it takes 10 min to reach the steady state. Dashed circles indicate the position of TE components. Black/white color indicates that the cloak is switched off/on, respectively.

the temperature profile, simply because still air is almost a thermal insulator. The thick green temperature contour line (about 32.5 °C) indicates the position where the temperature reaches its mid-value between the hot and cold ends of the plate. This line now locates closer to the hot end instead of lying in the middle of the plate, because of the heat blocking effect from the air hole. The asymmetric position of the air hole is chosen to facilitate the observation of this shift in temperature. In contrast, when the cloak is in operation, heat diffuses smoothly with a restored homogeneous temperature profile (Fig. 2(c)). The thick green temperature contour line (about 32.5 °C) also returns to its original position. This temperature profile is almost identical to the case when the air hole is absent (Fig. 2(a)), indicating that thermal invisibility has been achieved. There are still perceivable defects around the cloaked region with slight temperature distortion. These defects are because of the finite size of TE components.

We then proceed to demonstrate the controllable functionality of switching on/off for this thermal cloak in a dynamic.[31] In the beginning, the thermal cloak is switched off when heat diffuses from the hot end to the cold end of the Carbon Steel plate, reaching thermal equilibrium in about 10 min. Then the thermal cloak is switched on, restoring the homogeneous temperature profile. After another 10 min, the thermal cloak is switched off again. The temperature profiles at different time frames are extracted for illustration as in Fig. 3. It can be seen that, when the thermal cloak is switched off (Fig. 3(a)), the situation is similar to that without any cloak (Fig. 2(b)). In contrast, when the cloak is switched on, the temperature profile restores its homogeneity, realizing thermal invisibility (Fig. 3(b)). When the thermal cloak is switched off again, the temperature profile returns to the distorted one (Fig. 3(c)). This off-on-off process demonstrates clearly the dynamic switching functionality of the active thermal cloak.

Apart from on/off switching, another unique feature of this active thermal cloak is that it can apply to different geometries without rebuilding its constituents. To demonstrate this feature, a rectangular air hole with dimensions of 60.0×40.0 mm is chosen as the object to be cloaked in the same Carbon Steel plate. Previously, in order to hide a similar square object, cloaks based on coordinate transformation

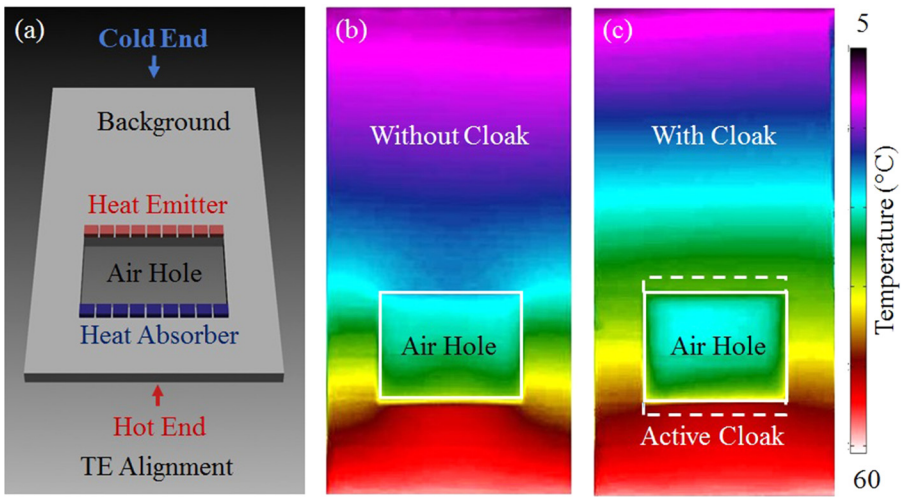

FIG. 4. Realization of thermal invisibility of a rectangular air hole in a metal plate. (a) Illustration of the alignment of TE components at two edges of the rectangular air hole in the Carbon Steel plate. Heat flux diffuses from bottom to top. (b) Temperature distortion caused by the rectangular air hole. (c) Homogeneous temperature profile restored by the active cloak. Dashed lines indicate the position of TE components.

required highly anisotropic and inhomogeneous metamaterials that are challenging to implement. In contrast, the active thermal cloak here can easily change its shape by re-aligning TE components along the upper/lower edges of the rectangle hole (Fig. 4(a)). With this setup, the blocked path of heat channel can be re-connected by TE components, allowing heat flux to diffuse uniformly in the remaining region out of the rectangular air hole. The performance of this thermal cloak is demonstrated in Figs. 4(b) and 4(c). When the rectangular air hole is embedded in the plate without any cloak, the air hole blocks heat diffusion and causes the temperature distortion (Fig. 4(b)). In contrast, when the rectangular air hole is cloaked, the temperature profile becomes homogeneous as if the air hole were not there (Fig. 4(c)). For objects with other geometries beside circles and rectangles, active thermal cloaking can also be realized using the same principle.

In conclusion, we present the design and implementation of active thermal cloaks that are made of TE components. With proper input voltages, TE components can "pump" heat from one side to the other side of the cloaked region, shielding the object in the heat channel. The effectiveness of active cloaking is experimentally demonstrated on a circular object and a rectangular object. This thermal cloaking approach incorporates active components in thermal metamaterial devices and brings dynamic controllability that is desirable in many applications.

This work was sponsored by Nanyang Technological University under Start-Up Grants, the Singapore Ministry of Education under Grant Nos. Tier 1 RG27/12 and MOE2011-T3-1-005.

[1]A. Alù and N. Engheta, Phys. Rev. E **72**(1), 016623 (2005).
[2]D. Schurig, J. J. Mock, B. J. Justice, S. A. Cummer, J. B. Pendry, A. F. Starr, and D. R. Smith, Science **314**(5801), 977 (2006).
[3]R. Liu, C. Ji, J. J. Mock, J. Y. Chin, T. J. Cui, and D. R. Smith, Science **323**(5912), 366 (2009).
[4]J. Valentine, J. Li, T. Zentgraf, G. Bartal, and X. Zhang, Nat. Mater. **8**(7), 568 (2009).
[5]L. H. Gabrielli, J. Cardenas, C. B. Poitras, and M. Lipson, Nat. Photonics **3**(8), 461 (2009).
[6]F. G. Vasquez, G. W. Milton, and D. Onofrei, Phys. Rev. Lett. **103**(7), 073901 (2009).
[7]B. Edwards, A. Alù, M. G. Silveirinha, and N. Engheta, Phys. Rev. Lett. **103**(15), 153901 (2009).
[8]H. F. Ma and T. J. Cui, Nat. Commun. **1**, 21 (2010).
[9]T. Ergin, N. Stenger, P. Brenner, J. B. Pendry, and M. Wegener, Science **328**(5976), 337 (2010).
[10]B. Zhang, Y. Luo, X. Liu, and G. Barbastathis, Phys. Rev. Lett. **106**(3), 033901 (2011).
[11]X. Chen, Yu. Luo, J. Zhang, K. Jiang, J. B. Pendry, and S. Zhang, Nat. Commun. **2**, 176 (2011).
[12]S. Narayana and Y. Sato, Adv. Mater. **24**(1), 71 (2012).
[13]F. Gömöry, M. Solovyov, J. Šouc, C. Navau, J. Prat-Camps, and A. Sanchez, Science **335**(6075), 1466 (2012).
[14]Q. Ma, Z. L. Mei, S. K. Zhu, T. Yu. Jin, and T. J. Cui, Phys. Rev. Lett. **111**(17), 173901 (2013).
[15]H. Chen, B. Zheng, L. Shen, H. Wang, X. Zhang, N. I. Zheludev, and B. Zhang, Nat. Commun. **4**, 2652 (2013).
[16]G. W. Milton, M. Briane, and J. R. Willis, New J. Phys. **8**(10), 248 (2006).
[17]H. Chen and C. T. Chan, Appl. Phys. Lett. **91**(18), 183518 (2007).
[18]F. G. Vasquez, G. W. Milton, and D. Onofrei, Wave Motion **48**(6), 515 (2011).
[19]S. Zhang, C. Xia, and N. Fang, Phys. Rev. Lett. **106**(2), 024301 (2011).
[20]S. Guenneau, C. Amra, and D. Veynante, Opt. Express **20**(7), 8207 (2012).
[21]S. Narayana and Y. Sato, Phys. Rev. Lett. **108**(21), 214303 (2012).
[22]E. M. Dede, T. Nomura, P. Schmalenberg, and J. S. Lee, Appl. Phys. Lett. **103**(6), 063501 (2013).
[23]Y. Ma, Lu. Lan, W. Jiang, F. Sun, and S. He, NPG Asia Mater. **5**, e73 (2013).
[24]R. Schittny, M. Kadic, S. Guenneau, and M. Wegener, Phys. Rev. Lett. **110**(19), 195901 (2013).
[25]T. Han, X. Bai, D. Gao, J. T. L. Thong, B. Li, and C.-W. Qiu, Phys. Rev. Lett. **112**(5), 054302 (2014).
[26]H. Xu, X. Shi, F. Gao, H. Sun, and B. Zhang, Phys. Rev. Lett. **112**(5), 054301 (2014).
[27]Y. Zhang, H. Xu, and B. Zhang, AIP Adv. **5**(5), 053402 (2015).
[28]U. Leonhardt, Science **312**(5781), 1777 (2006).
[29]J. B. Pendry, D. Schurig, and D. R. Smith, Science **312**(5781), 1780 (2006).
[30]B. J. Huang, C. J. Chin, and C. L. Duang, Int. J. Refrig. **23**(3), 208 (2000).
[31]See supplementary material at http://dx.doi.org/10.1063/1.4930989 for the entire dynamic switching process.